Chemical Papers (2020) 74:1609–1619
https://doi.org/10.1007/s11696-019-01011-5

ORIGINAL PAPER

Molecular structure, FT-IR and NMR analyses of dihydrogen-bonded $B_3N_3H_6$···HM complexes: a DFT and MP2 approach

Parimala Devi Duraisamy[1] · Praveena Gopalan[2] · Abiram Angamuthu[1]

Received: 9 July 2019 / Accepted: 26 November 2019 / Published online: 5 December 2019

Abstract

A theoretical study on the intermolecular dihydrogen bonding (DHB) of ground state $B_3N_3H_6$···HM (Li, Na, and K) complexes were investigated by B3LYP and MP2 methods with 6-311++G** basis set. Thermodynamic parameters (entropy, enthalpy, heat capacity and Gibbs free energy) of the complexes were calculated at different temperatures in the gas phase. The vibrational analysis of N–H···H–M DHB bond formation reveals that the calculated N–H and M–H stretching frequencies undergo red and blue shifts, respectively. The calculated interaction energies correlate well with the geometrical parameters wherein the shortest H···H intermolecular distance is obtained for $B_3N_3H_6$···HK complex. The chemical shift of ^{1}H, ^{11}B and ^{15}N NMR predict large variation for $B_3N_3H_6$···HK complex which has large protonic hydrogen than the hydridic hydrogen. Furthermore, natural bond orbital and quantum theory of atoms in molecule analyses were carried out to explore the non-covalent interaction along with the molecular electrostatic potential to predict the reactive sites of electrophilic and nucleophilic attack.

Graphic abstract

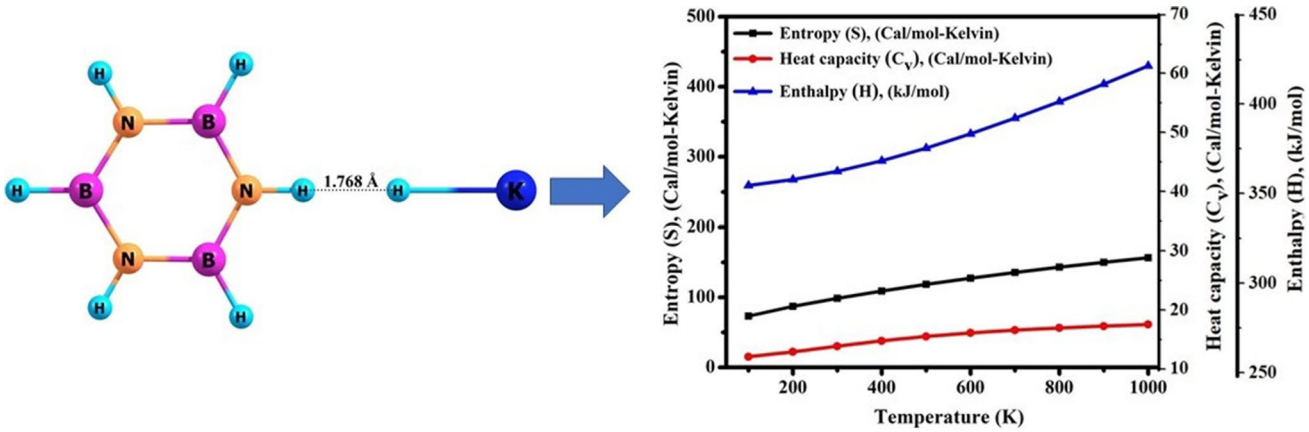

Keywords Dihydrogen bond · DFT · MP2 · Borazine · Metal hydrides · Molecular electrostatic potential

Electronic supplementary material The online version of this article (https://doi.org/10.1007/s11696-019-01011-5) contains supplementary material, which is available to authorized users.

✉ Abiram Angamuthu
aabiram@gmail.com

[1] Department of Physics, Karunya Institute of Technology and Sciences, Coimbatore, Tamilnadu 641114, India

[2] Department of Physics, PSGR Krishnammal College for Women, Coimbatore, Tamilnadu 641004, India

Introduction

In recent years hydrogen has received great attention in the research field due to its natural abundance, light weight, and minimum pollution (Gu et al. 2012; Payandeh Gharibdoust et al. 2018; Zhao et al. 2007; Zhao and Han 2012). Dihydrogen bonding (DHB) has sparked a considerable amount of interest over the past few decades, owing to their potential

application towards hydrogen storage (Ingram et al. 2018). The dihydrogen bonding is a special kind of conventional hydrogen bond arising from the closed approach of protonic and hydridic hydrogen atoms (Custelcean and Jackson 2001). It is generally denoted by X–H···H–M, wherein X–H is the proton donor (such as O–H or N–H) and H–M act as a proton acceptor (Lipkowski et al. 2004; Li et al. 2011). Generally, the H···H binding distance is less than or equal to sum of van der Waals radii of two hydrogen atoms (2.4 Å) and the X–H···H angle is found to be a linear arrangement (Planas et al. 2005). Numerous research groups have studied the dihydrogen-bonded complexes using thermodynamic parameters, spectroscopy, topological descriptors, and proton affinity measurements (Shubina et al. 1996; Ayllón et al. 2002; Belkova et al. 2007).

The first distinct affirmation for the formation of an intermolecular dihydrogen bond involving a metal hydride was proposed by Lee et al. (1994) and Lough et al. (1994). Experimentally, Wei et al. (2013) studied the dihydrogen bond formation between 2-pyridone and borane-trimethylamine (BTMA) complex in the gas phase and found the N–H···H–B dihydrogen bond formation to be at a distance of 1.78 Å using electronic and vibrational spectroscopy. Patwari et al. (2002) demonstrated the dihydrogen bonding in the cluster of borane-amines (BTMA) with phenol and aniline. They observed that the O–H···$(H–B)_2$ bond has smaller DHB distance than the N–H···H–B bond. The matrix isolation infrared spectroscopy and ab-initio calculation of various confirmation of $B_3N_3H_6$ dimer were performed by Verma and Viswanathan (2017) and they experimentally found the presence of T-shaped and dihydrogen-bonded dimer. Ramnial et al. (2003) studied imidazol-2-ylidene borane complex using X-ray crystallography and identified that N–H···H–B dihydrogen bond distance is shorter than that of C–H···H–B. An experimental review by Stennett and Harder (2016) report that various facets of S-block amidoboranes involve in the formation of N–H···H–B, B–H···H–B and N–H···H–N bonded interaction and they found applications in various disciplines, especially as hydrogen storage, reagents for the reduction of organic functional groups, catalysts and intermediates in dehydrocoupling reactions. The dehydrogenation reaction between phenol and borane-trimethylamine (BTMA) studied experimentally by Yang et al. (2015) further confirmed the existence of O–H···H–B bond.

Alkorta et al. (2010) theoretically studied the dihydrogen bond characteristics of the clusters of three aza-borane derivatives and concluded that the intermolecular dihydrogen bond distance becomes shorter with the increase in size of the cluster. Similarly, Yan et al. (2016) studied the dihydrogen-bonded amine–borane complexes in the appearance of N–H···H–B interactions and they identified that binding energy of the dimer gradually decreases as the number of substitution group increases. Zhao and Han (2007) have studied the infrared spectra of intermolecular dihydrogen-bonded phenol and borane trimethylamine complex using the time-dependent density functional theory method. They observed that the vibrational absorption bands of O–H and B–H stretching modes are strong in the ground state, whereas they disappeared in the excited state. Dihydrogen bond interaction between three ($C_2H_6N^+$) and four ($C_3H_8N^+$) membered ring cations with BeH_2 and MgH_2 studied by (Oliveira et al. 2010) confirm $C_2H_6N^+$ complex to provide stronger dihydrogen-bonded interactions.

Boron-based several experimental and theoretical studies are reported in the literature due to their potential application in hydrogen storage (Guo et al. 2010). Amongst them, Borazine ($B_3N_3H_6$) an inorganic analogue of benzene with three B–H and N–H alternative units is of great interest. Borazine and benzene are six-membered rings and both species possess similar physical properties. However, borazine is significantly less aromatic than benzene and chemical properties of borazine are slightly contrasted to its counterpart (Bagheri and Masoodi 2015; Verma et al. 2017). Borazine constitutes the new class of multifunctional, thermally stable materials with high electron and moderate hole mobilities for electroluminescent devices and hydrogen storage (Bettinger et al. 2009; Boshra et al. 2015). In many experimental literatures it is found that the light weight elements are feasible and able to achieve long-term goals for hydrogen storage owing to their high gravimetric and volumetric energy densities (Man et al. 2019). Hence, in this paper, we intend to study the dihydrogen-bonded interaction between $B_3N_3H_6$ with alkali metal hydrides (Li, Na, and K) using density functional theory and ab-initio methods. To understand the strength of interaction and type of bonding, interaction energy, natural bond orbital (NBO), quantum theory of atom in molecules (QTAIM) and molecular electrostatic potential (MEP) were analysed.

Computational details

The geometries of $B_3N_3H_6$···HM (M = Li, Na and K) complexes were computed at B3LYP (Lee et al. 1989; Becke 1996) and MP2 (Häser 1993) level of theory along with 6-311++G** basis set (Krishnan et al. 1980). The absence of imaginary frequency through vibrational analysis ensures that all the optimized geometries correspond to a minimum on the potential energy surface. From the frequency analysis, thermodynamic parameters were evaluated at 100–1000 K (in steps of 100 K) in the gas phase using B3LYP/6-311++G** level of theory (Güveli et al. 2010). The interaction energy of the considered complexes was calculated as the difference between the total energy (optimized) of the complex and sum of the individual energies of the

monomers and further corrections were made for basis set superposition error (BSSE) using the counterpoise method given below (Boys and Bernardi 1970)

$$\Delta E^{C} = E_{AB} - \left(E_{A} + E_{B}\right) + \text{BSSE} \quad (1)$$

where E_{AB} is the energy of the dihydrogen-bonded complexes formed between A and B molecules and E_A, E_B is the energy of individual monomers. Natural bond orbital (NBO) analysis was performed to examine the charge delocalization interaction and stability of molecule arising from hyper conjugative interactions (Reed et al. 1988). Bader's quantum theory of atom in molecule (QTAIM) (Bader 1991; Zheng et al. 2017) were carried out to understand the nature of interaction with the help of topological parameters using Multiwfn program (Lu and Chen 2012). In addition, molecular electrostatic potential (MEP) is used to find the reactive sites of the considered complexes (Bijina and Suresh 2016). All the quantum chemical calculations were performed using Gaussian 09 program (Frisch et al. 2009) and the structures were generated using ChemCraft ("Data Visualization Tools: ChemCraft" https://www.chemcraftprog.com) program package.

Results and discussion

Geometry and energies

The optimized molecular geometries of dihydrogen-bonded, $B_3N_3H_6\cdots$HM (M = Li, Na, K) complexes are depicted in Fig. 1.

The bond length of isolated monomers and their corresponding dihydrogen-bonded complexes were calculated using B3LYP and MP2 methods with 6-311++G** basis set and are listed in Tables 1 and 2. For better understanding the bond angles and dihedral angles of the complexes are given in Table S1 (supporting information).

Verma and Viswanathan (2017) experimentally demonstrated the dihydrogen-bonded interaction in borazine dimer and observed the H···H distance to be in the range of 2.13–2.46 Å. Here, for $B_3N_3H_6\cdots$HM (M = Li, Na and K) complexes, the H···H bond distances are found to be in the range of 1.728–1.827 Å and 1.607–1.801 Å at B3LYP and MP2 level of theory. All the obtained values are smaller than the sum of van der Waals radii of two hydrogen atoms (2.4 Å) and increases in the following

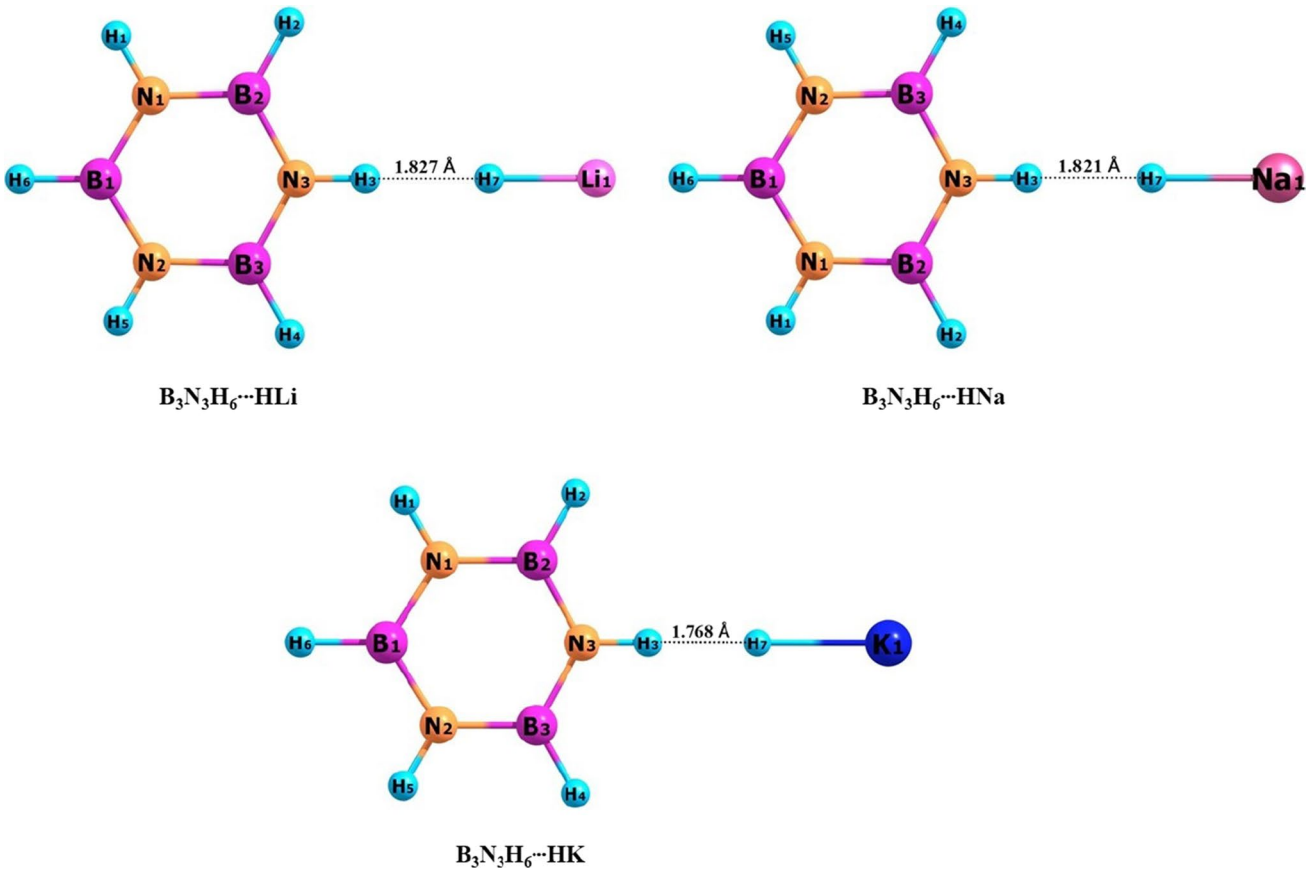

Fig. 1 Optimized structure of $B_3N_3H_6\cdots$HM (M = Li, Na, and K) complexes obtained at B3LYP/6-311++G** level of theory

Table 1 The bond length (Å) of isolated monomers calculated at B3LYP/6-311++G** and MP2/6-311++G** level of theories

Structure	B3LYP	MP2
$B_3N_3H_6$		
B–N	1.431	1.434
B–H	1.192	1.193
N–H	1.009	1.010
H–Li	1.593	1.599
H–Na	1.888	1.908
H–K	2.245	2.245

Table 2 The bond length of $B_3N_3H_6$···HM (M = Li, Na, K) complexes at B3LYP/6-311++G** and MP2/6-311++G** level of theories

Complexes		B3LYP	MP2
Bond length (Å)			
$B_3N_3H_6$···HLi	B2–N2	1.425	1.428
	B2–H2	1.194	1.195
	N3–H3	1.022	1.022
	H3···H7	1.827	1.801
	H7–Li1	1.588	1.595
$B_3N_3H_6$···HNa	B2–N2	1.425	1.427
	B2–H2	1.194	1.195
	N3–H3	1.023	1.025
	H3···H7	1.821	1.769
	H7–Na1	1.882	1.907
$B_3N_3H_6$···HK	B2–N2	1.423	1.434
	B2–H2	1.194	1.193
	N3–H3	1.029	1.055
	H3···H7	1.768	1.607
	H7–K1	2.241	2.299

order $B_3N_3H_6$···HK < $B_3N_3H_6$···HNa < $B_3N_3H_6$···HLi for both the levels. These results indicate that the interaction of $B_3N_3H_6$ with HK is comparatively better than that with HLi and HNa.

The calculated bond lengths of N–H for $B_3N_3H_6$···HM (M = Li, Na and K) complexes are 1.022–1.029 Å and 1.022–1.055 Å at B3LYP and MP2 levels. These are found to be elongated from the corresponding isolated monomer of $B_3N_3H_6$ (1.009 Å and 1.101 Å). For all the complexes, proton donors (N–H) are elongated upon complexation and the large elongation is observed for $B_3N_3H_6$···HK complex. On the other hand, the proton acceptor H–M (M = Li, Na, and K) is slightly shortened when compared to that of the isolated monomer. The bond length of all the complexes calculated at MP2 level is comparable with that of the B3LYP method. Reyes-márquez et al. (2008) studied the dihydrogen-bonded interaction for borane-oxaazacyclophane crystal structures and identified that linear X–H···H angle is appearing in the range of 150°–180° while H···H–Y bent angle is found around 95°–130°. In our case, the bond angle of all the complexes is found to be linear at both levels.

The optimized and interaction energies of $B_3N_3H_6$···HM (M = Li, Na, and K) complexes calculated at B3LYP and MP2 methods are shown in Table 3. The BSSE corrected interaction energy (ΔE^C) of the complexes is in the range of −4.317 to −5.779 kcal/mol and −4.832 to −5.886 kcal/mol for B3LYP and MP2, respectively. The result shows that intermolecular interaction energy follows the order of $B_3N_3H_6$···HK > $B_3N_3H_6$···HLi > $B_3N_3H_6$···HNa. These values are well matched with that of Grabowski et al. (2007), who reported the interaction energies to be in the range of −0.5 to −6.4 kcal/mol for their DHB systems having H···H bond length within 1.746–2.662 Å. $B_3N_3H_6$···HK complex which is identified to have the shortest H···H distance show comparatively larger interaction energy making it to be the better dihydrogen-bonded complex.

Vibrational frequencies

The vibrational frequencies of $B_3N_3H_6$ with HM (M = Li, Na, and K) and their respective isolates were calculated using the B3LYP/6-311++G** level of theory. Verma and Viswanathan (2017) experimentally studied the dihydrogen bonding in borazine dimer and observed that the N–H symmetric and asymmetric stretching vibrations are in the region of 3472 cm^{-1} and 3458 cm^{-1}, respectively. Theoretically calculated N–H stretching vibration frequency of the H···H bonded amine borane complex by Yan et al. (2016) is found to be 3533 cm^{-1}. Here, the calculated N–H symmetric stretching vibration for $B_3N_3H_6$···HM (M = Li, Na and K) complexes are found to be 3263–3396 cm^{-1} which is downward shifted by 232–365 cm^{-1} from the corresponding $B_3N_3H_6$ (3628 cm^{-1}) monomer, thereby confirming shift towards the red region. Large shift was observed for $B_3N_3H_6$···HK complex which is found to have large interaction energy. The N–H asymmetric stretching vibration for all the complexes is observed in the region of 3631 cm^{-1} and they are almost similar to its isolates. The observed values slightly vary from the reported literature which may be due to the unscaled vibration.

Oliveira (2012) study on binary and ternary complexes identified the H···H stretching vibration to be in the region

Table 3 Total energy (E_{tot}) and BSSE corrected interaction energies (ΔE^C) of $B_3N_3H_6$···HM (*M* = Li, Na, and K) complexes

Complexes	E_{tot}		ΔE^C (kcal/mol)	
	B3LYP	MP2	B3LYP	MP2
$B_3N_3H_6$···HLi	−250.84	−250.02	−4.373	−4.832
$B_3N_3H_6$···HNa	−405.61	−404.41	−4.317	−5.334
$B_3N_3H_6$···HK	−843.25	−842.10	−5.779	−5.886

of 40–160 cm^{-1}. In the same way, the H···H frequency for $B_3N_3H_6$···HM (M = Li, Na, K) complexes are in the range of 78–144 cm^{-1}. The $B_3N_3H_6$···HK complex has the least H···H stretching frequency value and these correlate well with the studies reported earlier (Li et al. 2011; Oliveira 2012). The HLi and HNa stretching vibrations are theoretically predicted by Alkorta et al. (2002) and Oliveira (2012) for dihydrogen-bonded complexes and respective vibrations are in the range of 1400–1500 cm^{-1} and 1000–1300 cm^{-1}. Li et al. (2011) theoretically studied the dihydrogen-bonded interaction in HB=BH···HK complex and observed that the HK stretching vibrations appear in the region of 1000–1100 cm^{-1}. In our complexes, the HLi and HNa symmetric stretching vibrations are observed at 1466 cm^{-1} and 1240 cm^{-1} and are blue shifted from the corresponding monomers (HLi = 1408 cm^{-1} and HNa = 1167 cm^{-1}). Similarly, for $B_3N_3H_6$···HK complex, the HK stretching vibration frequency is observed at 1076 cm^{-1} which is increased by 99 cm^{-1} from that of the HK monomer. Out of all the complexes, largest blue shift is observed for HK interacting $B_3N_3H_6$ complex which further agrees with the structural parameter of larger H–M bond distance.

Thermodynamic parameters

Thermodynamic parameters of $B_3N_3H_6$···HM (M = Li, Na, K) complexes were analysed at different temperatures (100–1000 K) using B3LYP/6-311++G** level of theory. The standard statistical thermodynamic functions namely entropy (S), heat capacity (C_v), enthalpy (H) and Gibbs free energy (G) were calculated. To understand the thermodynamic function, graph is plotted between different temperature versus entropy, heat capacity, enthalpy and Gibbs free energy and are depicted in Fig. 2a–d.

The thermodynamic function increases in positive coefficient basis with the increase in temperature from 100 to 1000 K. This may be due to the elevation of the molecular vibration intensity with respect to temperature. The specific heat capacity of the considered system gets decreased at low temperatures thereby obeying Debye T^3 law. However, the specific heat capacity of the complexes gets saturated at high temperatures (Durga et al. 2016). Zierkiewicz and Hobza (2004) studied the dihydrogen bonding in X_3CH···HM complexes and stated that the negative Gibbs free energies are stable. Liu and Yan (2018) observed that the Gibbs free

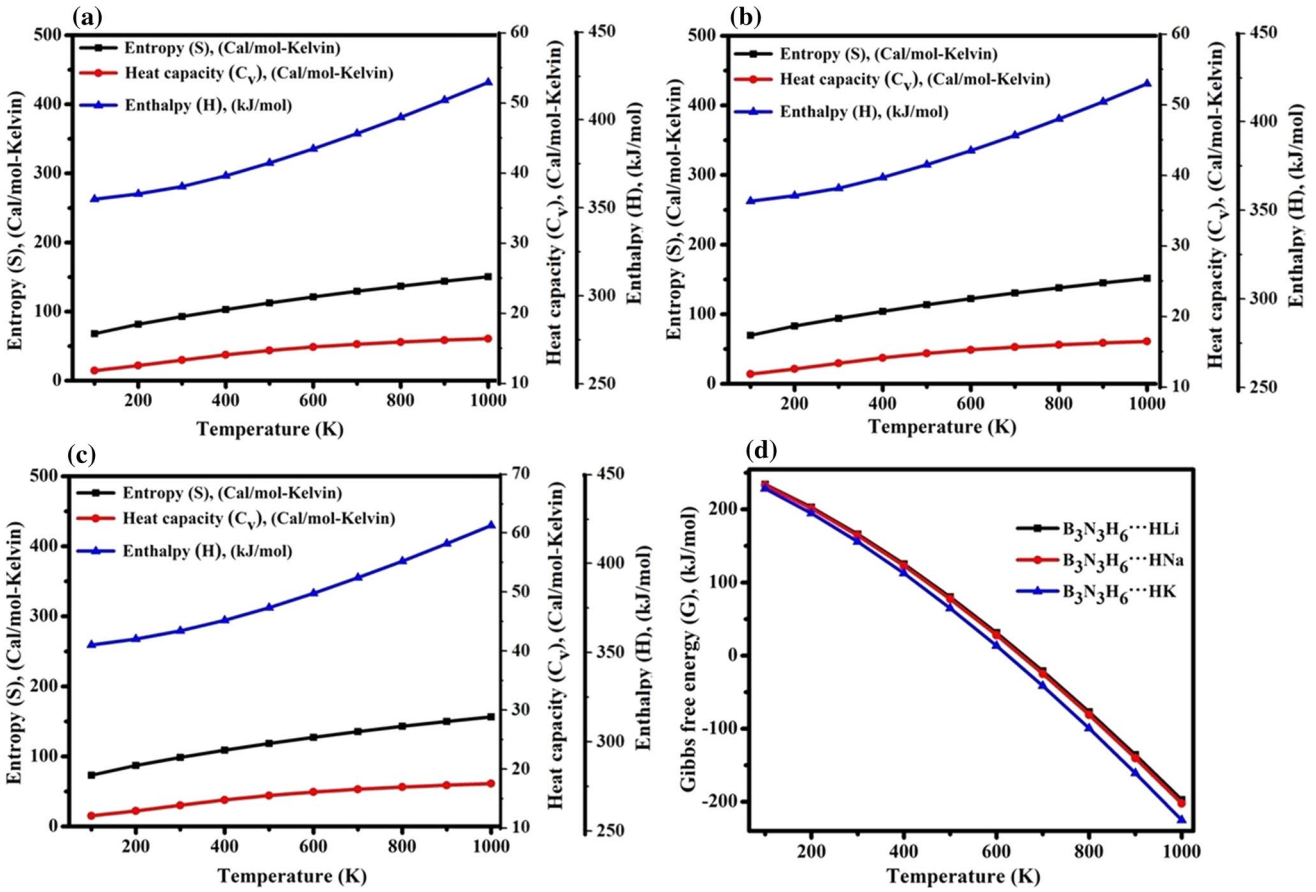

Fig. 2 Correlation graph of thermodynamic functions (S, C_v and H) and temperature for **a** $B_3N_3H_6$···HLi, **b** $B_3N_3H_6$···HNa, **c** $B_3N_3H_6$···HK and **d** Dependence of Gibbs free energy (G) versus temperature

energy decreases with an increase in the temperature for dihydrogen-bonded amine borane complexes and further found the dehydrogenation process to occur at higher temperatures. Figure 2d illustrates that the Gibbs free energy decreases as the temperature increases and their values are positive up to 600 K which reveals that the formed complexes are not spontaneous. At higher temperatures (700–1000 K), Gibbs free energy is negative in the range of − 21.18 to − 224.9 kcal/mol for all the complexes which further confirms the spontaneous reaction. The variation of the thermodynamic parameters is linear and sustained up to the maximum temperature confirming that the complexes are highly stable.

NMR spectra

The chemical shift of ^{1}H, ^{11}B and ^{15}N NMR for isolates and their complexes were obtained using gauge independent atomic orbitals (GIAO) at B3LYP/6-311++G** level of theory and the corresponding results are listed in Table 4.

Wei et al. (2016) experimentally studied the ^{1}H NMR for six membered borazine derivatives and observed them to be in the range of 1.18–6.33 ppm. In our study, the ^{1}H NMR of isolated borazine monomer is within the range of 4.921–5.440 ppm and correlates well with the previous work. On adding metal hydrides, ^{1}H NMR chemical shifts are in the range of 4.842–10.71 ppm for all the dihydrogen-bonded complexes. Most of the protons (H1, H2, H4–H7) are having lower chemical shift between 4.842 and 6.630 ppm because of the shielding effect, while protonic H3 atom have large chemical shift (8.694–10.71 ppm) due to deshielding effect. Alkorta et al. (2006) studied the dihydrogen bond interaction between $(XH)_2$, X = Li, Na, BeH, and MgH and HCN, HNC, and HCCH complexes and observed that protonic hydrogen is larger than the hydridic hydrogen atoms. Similarly, compared to the monomer, the chemical shift of protonic H3 atom is increased largely due to the contribution of electronegative atom (N3) and metal hydride. This large variation of chemical shift (H3 atom) is observed for $B_3N_3H_6\cdots HK$ complex. The chemical shift of H3 atom varies in the order of $B_3N_3H_6\cdots HLi < B_3N_3H_6\cdots HNa < B_3N_3H_6\cdots HK$ among the complexes. Gervais et al. (2005) experimentally studied boron nitride preceramic polymer using NMR analysis and observed ^{11}B NMR spectrum of B(III) coordinated atoms to be within the range of 0–40 ppm. Here, ^{11}B NMR chemical shift of isolated monomer are in the range of 10.282–10.345 ppm and these values are well matched with the earlier reported results (Gervais et al. 2005). The chemical shift of ^{11}B and ^{15}N NMR of the complexes are found to be in the range of 9.490–9.830 ppm and 138.9–163.7 ppm, respectively. A similar trend as that of H3 atom is observed for N3 wherein more shift is observed for $B_3N_3H_6\cdots HK$ complex.

Table 4 The ^{1}H, ^{11}B and ^{15}N NMR of isolates and their complexes calculated at B3LYP/6-311++G** level of theory

Atoms	$B_3N_3H_6$	$B_3N_3H_6\cdots HLi$	$B_3N_3H_6\cdots HNa$	$B_3N_3H_6\cdots HK$
N1	139.9	138.9	138.9	138.9
N2	139.9	138.9	138.9	138.9
N3	140.0	156.4	158.1	163.7
B1	10.345	9.679	9.603	9.490
B2	10.282	9.766	9.793	9.830
B3	10.282	9.766	9.795	9.830
H1	5.439	5.200	5.201	5.175
H2	4.921	4.842	4.859	4.9
H3	5.472	8.694	8.934	10.071
H4	4.921	4.842	4.860	4.9
H5	5.440	5.200	5.201	5.715
H6	4.950	4.854	4.859	4.865
H7	–	5.439	5.976	6.630

NBO and Mulliken charge analysis

The natural bond orbital (NBO) analysis provides an efficient method for studying intra and intermolecular interaction and provides the interaction between bonding (donor or lone pair) and antibonding orbitals (empty or acceptor). Second-order perturbation theory has been employed to estimate the stabilization energies of bonding and anti-bonding orbitals. The delocalization interaction or donor acceptor charge transfers can be evaluated from the off diagonal fock matrix element. The NBO analysis were performed for $B_3N_3H_6\cdots HM$ (M = Li, Na, and K) complexes at the B3LYP/6-311++G** level of theory. The calculated stabilization energy, energy difference between donor and acceptor orbitals $[E(j) - E(i)]$ and the element of Fock matrix ($F(i,j)$) are listed in Table 5.

The stabilization energy $E(2)$ of the considered complexes are calculated to be in the range of 10.01–17.34 kcal/mol and the charge transfer is between bonding orbital of σ (H7–Na1) or LP (H7) and antibonding orbital of σ*(N3–H3) bond. Earlier (Yao and Ren 2011) studied the

Table 5 NBO analysis of $B_3N_3H_6\cdots HM$ (M = Li, Na, and K) complexes performed at B3LYP/6-311++G** level of theory

Complexes	Donor (i)	Acceptor (j)	$E(2)$ (kcal/mol)	$E(j) - E(i)$ (a.u.)	$F(i,j)$ (a.u.)
$B_3N_3H_6\cdots HLi$	LP (H7)	σ* (N3–H3)	13.25	0.69	0.089
$B_3N_3H_6\cdots HNa$	σ (H7–Na1)	σ* (N3–H3)	10.01	0.71	0.076
$B_3N_3H_6\cdots HK$	LP(H7)	σ* (N3–H3)	17.34	0.67	0.100

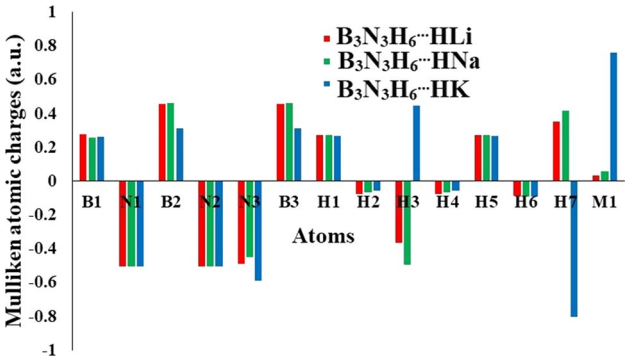

Fig. 3 Mulliken charge distribution in $B_3N_3H_6$···HM (M = Li, Na, and K) obtained at B3LYP/6-311++G** level of theory

DHB in HB=BH···HM (M = Li, Na and K) complexes and identified that HK involved complexes have more stabilization energy than HLi and HNa. In our study also the stabilization energy ($E(2)$) of $B_3N_3H_6$···HK is larger (17.34 kcal/mol) comparatively and agrees with the earlier reports. The order of stabilization energy of the complex is $B_3N_3H_6$···HK > $B_3N_3H_6$···HLi > $B_3N_3H_6$···HNa.

The atomic charge of the considered complexes was obtained at B3LYP/6-311++G** level of theory and the corresponding charge distribution graph is depicted in Fig. 3.

The atomic charge plays a vital role in the utilization of quantum mechanical calculations to the molecular system. Charge distribution is calculated by determining the electron population of each atom as defined by the basis function. From the charge distribution of present complexes, it is observed that the boron attached with hydrogen atom is positive except for H3 atom in Li and Na containing complex which may be due to the weakest interaction between the H···H bonds. However, for KH complex, the H3 atom has a positive charge exhibiting strong H···H interaction compared to Li and Na metal hydrides. From Mulliken charge analysis, the obtained atomic charge unveils that KH atoms have the highest positive charge whereas H7 atom accommodates more negative charges than other atom. This indicates that H7 atom is more negatively charged, and hence can easily interact with the donor atom.

QTAIM analysis

The Bader's quantum theory of atom in molecules (QTAIM) is a pioneer tool to understand the nature of interactions for various molecular systems. The topological parameters such as electron density (ρ), Laplacian of electron density ($\nabla^2\rho$), ellipticity (ε), kinetic (G_C), potential (V_C), and sum of their total electronic energy density (H_C), are evaluated at B3LYP/6-311++G** level of theory and listed in Table 6.

The QTAIM molecular graph of $B_3N_3H_6$···HM (M = Li, Na and K) complexes is shown in Fig. 4.

The electron density (ρ) and Laplacian of electron density ($\nabla^2\rho$) at bond critical points (*bcp*) for all the complexes fall in the range of 0.0175–0.0211 a.u. and 0.0359–0.0372 a.u., respectively, and are similar to the range reported by Grabowski et al. (2007). To understand the bonding strength, graph is plotted between dihydrogen bond distance ($d_{H\cdots H}$) and electron density (ρ) and depicted in Fig. 5. Sandhya et al. (2018) identified that the DHB distance increases as the strength of electron density decreases (ρ). A similar correlation is observed between these two parameters as seen from Fig. 5.

Generally, sign of $\nabla^2\rho$ indicates the types of bonding: positive values determine closed shell system or non-covalent

Table 6 Topological parameters (in a.u.) of the complexes calculated at B3LYP/6-311++G** level of theory

Complexes	ρ	$\nabla^2\rho$	G_C	V_C	$-G_C/V_C$	H_C	ε
$B_3N_3H_6$···HLi	0.0175	0.0359	0.0083	−0.0076	1.0921	0.0007	0.0189
$B_3N_3H_6$···HNa	0.0181	0.03498	0.0083	−0.0078	1.0641	0.0004	0.0176
$B_3N_3H_6$···HK	0.0211	0.03723	0.00935	−0.0094	0.9947	−0.00005	0.0154

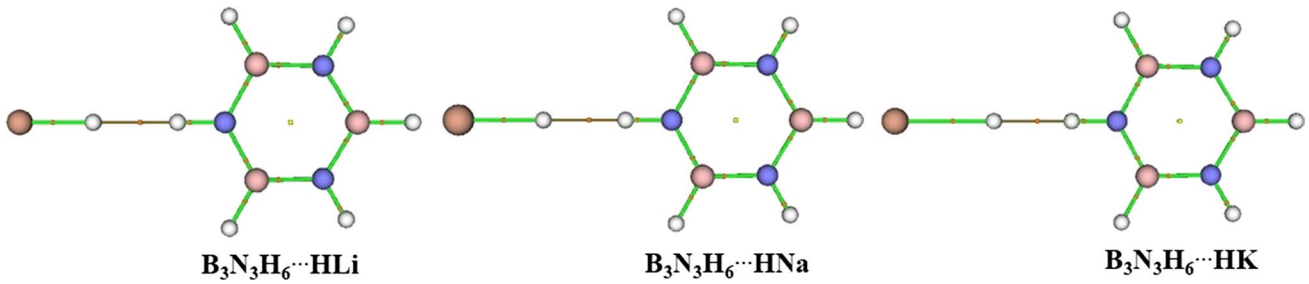

Fig. 4 The QTAIM molecular graph of $B_3N_3H_6$···HM (M = Li, Na, K) complexes obtained at B3LYP/6-311++G** level of theory. Yellow circles denote bond paths

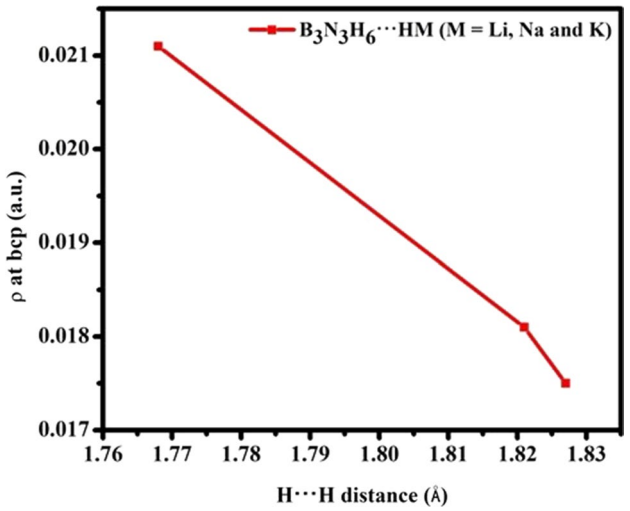

Fig. 5 Plot of the dihydrogen bond distance versus electron density at *bcp*

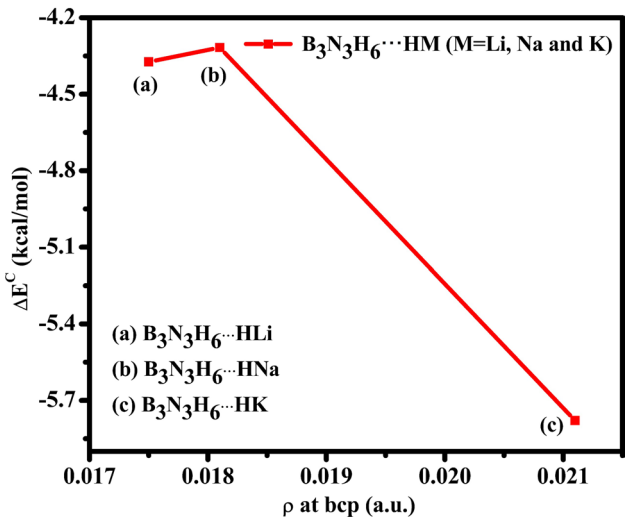

Fig. 6 Correlation graph between electron density and ΔE^{C}

interaction and negative values denote the covalent bond (Venkataramanan et al. 2018). Here, the ($\nabla^2\rho$) is positive for all the H···H bonded systems thereby confirming the existence of noncovalent type. Among all the complexes, the largest value of ρ and ($\nabla^2\rho$) is observed for $B_3N_3H_6$···HK. Figure 6 displays the correlation between the electron density and interaction energy (ΔE^{C}) wherein it is observed that ρ increases with the decrease in interaction energy. Venkataramanan et al. (2018) reported that if the ratio of $G_C/V_C > 1$ then the nature of interaction is non-covalent while $G_C/V_C < 1$ then the interaction is considered as covalent. The ratio of G_C/V_C and ε of the considered system are within the range of 0.995–1.092 a.u. and 0.015–0.019 a.u. which further confirms that all the complexes have non-covalent interaction.

Molecular electrostatic potential (MEP)

To understand the dihydrogen-bonded interaction between molecules, molecular electrostatic potential (MEP) analysis for $B_3N_3H_6$···HM complexes are carried out at B3LYP/6-311++G** level of theory and are depicted in Fig. 7.

MEP provides a visual method to understand the charge distribution of the molecule. Generally, the red-color surface represents the nucleophilic region, and the blue-color part denotes the electrophilic region. For all the complexes, blue and red regions are found to be M–H and N–H bonds and the green region is nearly equal to zero potential. From this result, N–H and M–H bonds clearly indicate strong and weak interaction, respectively. The MEP of $\Delta V_n(D)$, $\Delta V_n(A)$, $\Delta\Delta V_n$ and interaction energy of H···H (E_{nb}) are listed in Table 7.

The electron donating and accepting ability of donor and acceptor atoms are defined as $\Delta V_n(D)$, $\Delta V_n(A)$ and difference between donor $\Delta V_n(D)$ and acceptor $\Delta V_n(A)$ atoms are referred to as $\Delta\Delta V_n$. For all complexes, $\Delta V_n(D)$ and $\Delta V_n(A)$ specifies positive and negative bonds indicating that donor (D) donates electron density to acceptor

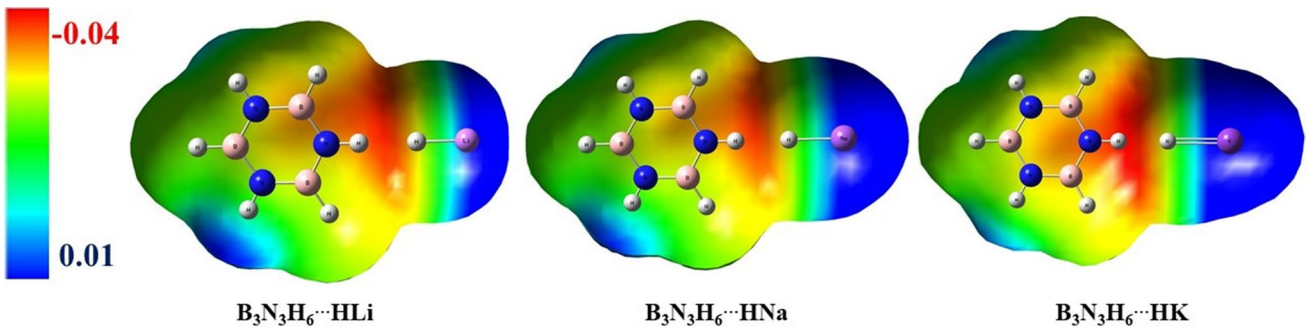

Fig. 7 The molecular electrostatic potential map for $B_3N_3H_6$···HM (M = Li, Na, and K) complexes calculated at B3LYP/6-311++G** level of theory

Table 7 MEP parameters for all the complexes calculated at B3LYP/6-311++G** level of theory

Complexes	$\Delta V_n(D)$ (a.u.)	$\Delta V_n(A)$ (a.u.)	$\Delta\Delta V_n$ (a.u.)	E_{nb} (kcal/mol)
$B_3N_3H_6\cdots$HLi	−0.8029	−5.4458	4.6428	−414.67
$B_3N_3H_6\cdots$HNa	−1.9065	−5.459	3.5525	−317.31
$B_3N_3H_6\cdots$HK	−2.8305	5.5292	2.6987	−241.08

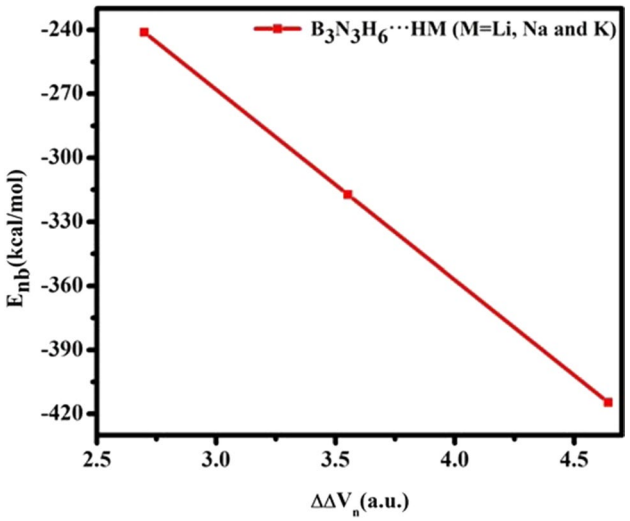

Fig. 8 Correlation between $\Delta\Delta V_n$ and interaction energy (E_{nb}) of the dihydrogen-bonded complexes

(*A*) during the dihydrogen bond formation. The $\Delta\Delta V_n$ and interaction energy E_{nb} of the complexes lie in the range of 2.699–4.643 a.u. and −241.08 to −414.67 kcal/mol, respectively. Mohan and Suresh (2014) in their study reported the electron donor–acceptor interaction (eDA) between donor and acceptor of non-covalent complexes (hydrogen, halogen and dihydrogen bond). To know the strength of donor and acceptor, graph (Fig. 8) is plotted between $\Delta\Delta V_n$ and interaction energy (E_{nb}) and they confirm that the dihydrogen bond strength is related to the donor–acceptor strength.

Conclusion

In this work dihydrogen-bonded complexes of $B_3N_3H_6$ with alkali metal hydrides (LiH, NaH, and KH) are investigated using B3LYP and MP2 with 6-311++G** basis set. The H···H distance of all the complexes suggests the existence of dihydrogen bonding and the most stable DHB distance was observed in $B_3N_3H_6\cdots$HK complex. The vibrational frequency analysis predicts the red and blue shifts to occur in N–H and M–H bonds, respectively, for all the complexes. Large interaction energy was observed for $B_3N_3H_6\cdots$HK complex having the smallest H···H distance thus confirming them to be the most suitable structure for DHB. ^{1}H, ^{15}N NMR study on the borazine isolate and its complexes predict more chemical shift for $B_3N_3H_6\cdots$HK. The correlation between Gibbs free energy and temperature shows that the complexes are spontaneous only in the temperature range of 700–1000 K in the gas phase. Moreover, the NBO analysis revealed that $B_3N_3H_6\cdots$HK complex has more stabilization energy (17.34 kcal/mol) between donor σ* (N–H) and acceptor LP (M–H). Topological parameters such as electron density (ρ) and positive values of Laplacian of electron density ($\nabla^2\rho$) indicate that all the complexes have non-covalent interaction. The results of this study may be helpful for understanding the dihydrogen-bonded interaction between borazine and alkali metal hydrides. This in the future may aid the researches involved in the design of borazine containing multi dihydrogen-bonded system for hydrogen storage applications.

Acknowledgements The authors are thankful to "Bioinformatics resources and applications facility (BRAF), C-DAC, Pune" for providing the computational facilities. Also, the authors would like to thank the Computer Technology Centre (CTC) in Karunya institute of technology and sciences, Coimbatore, India for offering the workstation to carry out this work.

References

Alkorta I, De J, Cier V et al (2002) Ab initio study of the structural, energetic, bonding, and IR spectroscopic properties of complexes with dihydrogen bonds. J Phys Chem A 106:9325–9330. https://doi.org/10.1021/jp021159w

Alkorta I, Zborowski K, Elguero J, Solimannejad M (2006) Theoretical study of dihydrogen bonds between $(XH)_2$, X = Li, Na, BeH, and MgH, and weak hydrogen bond donors (HCN, HNC, and HCCH). J Phys Chem A 110:10279–10286. https://doi.org/10.1021/jp061481x

Alkorta I, Blanco F, Elguero J (2010) Dihydrogen bond cooperativity in aza-borane derivatives. J Phys Chem A 114:8457–8462. https://doi.org/10.1021/jp1046694

Ayllón JA, Gervaux C, Sabo-Etienne S, Chaudret B (2002) First NMR observation of the intermolecular dynamic proton transfer equilibrium between a hydride and coordinated dihydrogen: $(dppm)_2HRuH\cdots H\text{–}OR{=}[(dppm)_2HRu(H_2)]^+(OR)^-$. Organometallics 16:2000–2002. https://doi.org/10.1021/om970079p

Bader RF (1991) A quantum theory of molecular structure and its applications. Chem Rev 91:893–928. https://doi.org/10.1021/cr00005a013

Bagheri S, Masoodi HR (2015) Theoretical study of the influence of cation-π and anion-π interactions on some NMR data of borazine complexes. Chem Phys Lett 629:46–52. https://doi.org/10.1016/j.cplett.2015.04.017

Becke AD (1996) Density-functional thermochemistry. IV. A new dynamical correlation functional and implications for

exact-exchange mixing. J Chem Phys 104:1040–1046. https://doi.org/10.1063/1.470829
Belkova NV, Dub PA, Baya M, Houghton J (2007) Kinetics and thermodynamics of proton transfer to Cp*Ru(dppe)H: via dihydrogen bonding and (η^2-H_2)-complex to the dihydride. Inorg Chim Acta 360:149–162. https://doi.org/10.1016/j.ica.2006.07.106
Bettinger HF, Kar T, Sánchez-García E (2009) Borazine and benzene homo and heterodimers. J Phys Chem A 113:3353–3359. https://doi.org/10.1021/jp808173h
Bijina PV, Suresh CH (2016) Molecular electrostatic potential analysis of non-covalent complexes. J Chem Sci 128:1677–1686. https://doi.org/10.1007/s12039-016-1162-5
Boshra A, Oliaey AR, Rezaie F et al (2015) Novel cations of xenon trifluoroborazine complexes: structures, reactivities, and natural bonding orbital analysis. J Fluor Chem 178:99–106. https://doi.org/10.1016/j.jfluchem.2015.07.013
Boys SF, Bernardi F (1970) The calculation of small molecular interactions by the differences of separate total energies. Some procedures with reduced errors. Mol Phys 19:553–566. https://doi.org/10.1080/00268977000101561
Chemcraft - graphical software for visualization of quantum chemistry computations. https://www.chemcraftprog.com
Custelcean R, Jackson JE (2001) Dihydrogen bonding: structures, energetics, and dynamics. Chem Rev 101:1963–1980. https://doi.org/10.1021/cr000021b
Durga R, Anand S, Rajkumar K et al (2016) The spectroscopic (FT-IR, FT-Raman, NMR & UV–Vis) order hyperpolarizability, homo and lumo analysis of maleic anhydride by HF and DFT methods. J Appl Pyhsics 8:1–14. https://doi.org/10.9790/4861-0803020114
Frisch MJ et al (2009) Gaussian 09 Revision B.01. Gaussian Inc., Wallingford
Gervais C, Framery E, Duriez C et al (2005) ^{11}B and ^{15}N solid state NMR investigation of a boron nitride preceramic polymer prepared by ammonolysis of borazine. J Eur Ceram Soc 25:129–135. https://doi.org/10.1016/j.jeurceramsoc.2004.07.010
Grabowski SJ, Sokalski WA, Leszczynski J (2007) Wide spectrum of H···H interactions: van der Waals contacts, dihydrogen bonds and covalency. Chem Phys 337:68–76. https://doi.org/10.1016/j.chemphys.2007.06.042
Gu Q, Gao L, Guo Y et al (2012) Structure and decomposition of zinc borohydride ammonia adduct: towards a pure hydrogen release. Energy Environ Sci 5:7590–7600. https://doi.org/10.1039/c2ee02485c
Guo Y, Xia G, Zhu Y et al (2010) Hydrogen release from amminelithium borohydride, $LiBH_4{\cdot}NH_3$. Chem Commun 46:2599–2601. https://doi.org/10.1039/b924057h
Güveli S, Özdemir N, Bal-Demirci T et al (2010) Quantum-chemical, spectroscopic and X-ray diffraction studies on nickel complex of 2-hydroxyacetophenone thiosemicarbazone with triphenylphospine. Polyhedron 29:2393–2403. https://doi.org/10.1016/j.poly.2010.05.004
Häser M (1993) Møller-Plesset (MP2) perturbation theory for large molecules. Theor Chim Acta 87:147–173. https://doi.org/10.1007/BF01113535
Ingram DJ, Headen TF, Skipper NT et al (2018) Dihydrogen: vs. hydrogen bonding in the solvation of ammonia borane by tetrahydrofuran and liquid ammonia. Phys Chem Chem Phys 20:12200–12209. https://doi.org/10.1039/c7cp08220g
Krishnan R, Binkley JS, Seeger R, Pople JA (1980) Self-consistent molecular orbital methods. XX. A basis set for correlated wave functions. J Chem Phys 72:650–654. https://doi.org/10.1063/1.438955
Lee C, Hill C, Carolina N (1989) Development of the Colle-Salvetti correlation-energy formula into a functional of the electron density. Chem Phys Lett 162:165–169. https://doi.org/10.1016/0009-2614(89)85118-8
Lee JC, Peris E, Rheingold AL, Crabtree RH (1994) An unusual type of H···H interaction: Ir–H···H–O and Ir–H···H–N hydrogen bonding and its involvement in σ-bond metathesis. J Am Chem Soc 116:11014–11019. https://doi.org/10.1021/ja00103a017
Li Y, Zhang L, Du S et al (2011) A MP2(full) and CCSD(T) theoretical investigation on the dihydrogen-bonded interactions between HNa and RB=BH (R = F, Cl, H, CN, NC and CO). Comput Theor Chem 977:201–208. https://doi.org/10.1016/j.comptc.2011.09.033
Lipkowski P, Grabowski SJ, Robinson TL, Leszczynski J (2004) Properties of the C–H···H dihydrogen bond: an ab initio and topological analysis. J Phys Chem A 108:10865–10872. https://doi.org/10.1021/jp048562i
Liu B, Yan S (2018) DFT investigation on the decomposition of dihydrogen-bonded methylamine-borane octamer. Comput Theor Chem 1127:1–7. https://doi.org/10.1016/j.comptc.2018.01.018
Lough AJ, Park S, Ramachandran R, Morris RH (1994) Switiching on and off a new intramolecular hydrogen–hydrogen interaction and the heterolytic splitting of dihydrogen. J Am Chem Soc 116:8356–8357. https://doi.org/10.1021/ja00097a049
Lu T, Chen F (2012) Multiwfn: a multifunctional wavefunction analyzer. J Comput Chem 33:580–592. https://doi.org/10.1002/jcc.22885
Man HW, Tsang CS, Li MMJ et al (2019) Transition metal-doped nickel phosphide nanoparticles as electro- and photocatalysts for hydrogen generation reactions. Appl Catal B Environ 242:186–193. https://doi.org/10.1016/j.apcatb.2018.09.103
Mohan N, Suresh CH (2014) A molecular electrostatic potential analysis of hydrogen, halogen, and dihydrogen bonds. J Phys Chem A 118:1697–1705. https://doi.org/10.1021/jp4115699
Oliveira BG (2012) Interplay between dihydrogen and alkali-halogen bonds: is there some covalency upon complexation of ternary systems? Comput Theor Chem 998:173–182. https://doi.org/10.1016/j.comptc.2012.07.031
Oliveira BG, Araújo RCMU, Carvalho AB, Ramos MN (2010) A theoretical study of dihydrogen bonds in small protonated rings : aziridine and azetidine cations. Spectrochim Acta Part A Mol Biomol Spectrosc 75:563–566. https://doi.org/10.1016/j.saa.2009.11.017
Patwari GN, Ebata T, Mikami N (2002) Gas phase dihydrogen bonding: clusters of borane-amines with phenol and aniline. Chem Phys 283:193–207. https://doi.org/10.1016/S0301-0104(02)00529-3
Payandeh Gharibdoust S, Heere M, Nervi C et al (2018) Synthesis, structure, and polymorphic transitions of praseodymium(iii) and neodymium(iii) borohydride, $Pr(BH_4)_3$ and $Nd(BH_4)_3$. Dalt Trans 47:8307–8319. https://doi.org/10.1039/c8dt00118a
Planas JG, Viñas C, Teixidor F et al (2005) Self-assembly of mercaptane-metallacarborane complexes by an unconventional cooperative effect: a C–H···S–H···H–B hydrogen/dihydrogen bond interaction. J Am Chem Soc 127:15976–15982. https://doi.org/10.1021/ja055210w
Ramnial T, Jong H, McKenzie ID et al (2003) An imidazol-2-ylidene borane complex exhibiting inter-molecular [C–HΔ^+···HΔ^-–B] dihydrogen bonds. Chem Commun 3:1722–1723. https://doi.org/10.1039/b301416a
Reed AE, Curtiss LA, Weinhold F (1988) Intermolecular interactions from a natural bond orbital, donor–acceptor viewpoint. Chem Rev 88:899–926. https://doi.org/10.1021/cr00088a005
Reyes-márquez V, Lara O, Sánchez M (2008) Unconventional hydrogen and dihydrogen bonded supramolecular array of a 2,6-dioxa-9,16-diaza-1,3(1,2),4(1,4) tribenzenacycloheptadecaphane-borane adduct. Arkivoc. https://doi.org/10.3998/ark.5550190.0009.510
Sandhya KS, Remya GS, Suresh CH (2018) Special issue on modern trends in inorganic chemistry intermolecular dihydrogen bonding in VI, VII, and VIII group octahedral metal hydride complexes

with water. J Chem Sci 130:1–8. https://doi.org/10.1007/s12039-018-1498-0

Shubina ES, Belkova NV, Krylov AN et al (1996) Spectroscopic evidence for intermolecular M–H···H–OR hydrogen bonding: interaction of $WH(CO)_2(NO)L_2$ hydrides with acidic alcohols. J Am Chem Soc 118:1105–1112. https://doi.org/10.1021/ja953094z

Stennett TE, Harder S (2016) S-block amidoboranes: syntheses, structures, reactivity and applications. Chem Soc Rev 45:1112–1118. https://doi.org/10.1039/c5cs00544b

Venkataramanan NS, Suvitha A, Kawazoe Y (2018) Density functional theory study on the dihydrogen bond cooperativity in the growth behavior of dimethyl sulfoxide clusters. J Mol Liq 249:454–462. https://doi.org/10.1016/j.molliq.2017.11.062

Verma K, Viswanathan KS (2017) The borazine dimer: the case of a dihydrogen bond competing with a classical hydrogen bond. Phys Chem Chem Phys 19:19067–19074. https://doi.org/10.1039/c7cp04056c

Verma K, Viswanathan KS, Majumder M, Sathyamurthy N (2017) How different is the borazine–acetylene dimer from the benzene–acetylene dimer? A matrix isolation infrared and ab initio quantum chemical study. Mol Phys 115:2637–2648. https://doi.org/10.1080/00268976.2017.1284357

Wei N, Hamza A, Hao C et al (2013) Time-dependent density functional theory study on hydrogen and dihydrogen bonding in electronically excited state of 2-pyridone–borane–trimethylamine cluster. J Clust Sci 24:459–470. https://doi.org/10.1007/s10876-013-0572-5

Wei D, Chen L, Xu T et al (2016) Synthesis and characterization of a novel borazine-type UV photo-induced polymerization of ceramic precursors. Molecules 21:1–11. https://doi.org/10.3390/molecules21060801

Yan S, Zou H, Kang W, Sun L (2016) DFT investigation on dihydrogen-bonded amine-borane complexes. J Mol Model 22:1–10. https://doi.org/10.1007/s00894-015-2886-8

Yang Y, Liu Y, Yang D et al (2015) Theoretical study on the dehydrogenation reaction of dihydrogen bonded phenol–boranetrimethylamine in the excited state. Phys Chem Chem Phys 17:32132–32139. https://doi.org/10.1039/C5CP02530C

Yao AQ, De Ren F (2011) A MP2 and CCSD(T) theoretical investigation on the weak dihydrogen-bonded interactions between HB=BH ($1\Delta g$) and HM (M = Li, Na, K, BeH, MgH or CaH). Comput Theor Chem 963:463–469. https://doi.org/10.1016/j.comptc.2010.11.014

Zhao GJ, Han KL (2012) Hydrogen bonding in the electronic excited state. Acc Chem Res 45:404–413. https://doi.org/10.1021/ar200135h

Zhao GJ, Han KL (2007) Novel infrared spectra for intermolecular dihydrogen bonding of the phenol–borane–trimethylamine complex in electronically excited state. J Chem Phys 127:024306. https://doi.org/10.1063/1.2752808

Zhao GJ, Liu JY, Zhou LC, Han KL (2007) Site-selective photoinduced electron transfer from alcoholic solvents to the chromophore facilitated by hydrogen bonding: a new fluorescence quenching mechanism. J Phys Chem B 111:8940–8945. https://doi.org/10.1021/jp0734530

Zheng D, Zhang M, Zhao G (2017) Combined TDDFT and AIM insights into photoinduced excited state intramolecular proton transfer (ESIPT) mechanism in hydroxyl- and amino-anthraquinone solution. Sci Rep 7:1–10. https://doi.org/10.1038/s41598-017-14094-5

Zierkiewicz W, Hobza P (2004) The dihydrogen bond in X_3C–H···H–M complexes (X = F, Cl, Br; M = Li, Na, K). A correlated quantum chemical ab initio and density functional theory study. Phys Chem Chem Phys 6:5288–5296. https://doi.org/10.1039/B410112J